Supporting Information

Regulating the Structural Dimensionality, Gas Sorption and Magnetic Behavior of Co(II) Coordination Polymers

Sujeet Kumar Pal,[a] Dhanajay Tiwari,[a] Madan Mohan,[a] Ahmad Husain*[b] Ajit Kumar Kharwar*[a]

[a.] Department of chemistry, Banaras Hindu University, Varanasi, U.P.-221005, India E-mail: akkharwar.chem@bhu.ac.in
[b.] Department of Chemistry, DAV University, Jalandhar, Punjab-144012, India E-mail: ahmad.husain@outlook.com

Table S1

Identification code	1	2	3
Empirical formula	$C_{60}H_{50}Co_4N_6O_{18}$	$C_{34}H_{33}Co_2N_3O_9$	$C_{78}H_{57}Co_2N_7O_{10}$
Formula weight	1378.78	745.49	1370.16
Temperature/K	293.15	176(100)	133.77
Crystal system	monoclinic	triclinic	triclinic
Space group	$P2_1/n$	P-1	P-1
a/Å	6.8851(3)	8.5731(5)	14.6443(13)
b/Å	14.5259(7)	13.2356(7)	16.4598(15)
c/Å	27.3637(12)	15.4444(8)	16.4623(15)
α/°	90	114.010(5)	100.736(5)
β/°	94.163(5)	102.728(5)	114.653(4)
γ/°	90	91.420(5)	97.526(5)
Volume/Å^3	2729.5(2)	1548.57(16)	3445.2(6)
Z	2	2	2
ρ_{calc}g/cm^3	1.678	1.599	1.321
μ/mm^{-1}	1.280	1.134	0.547
F(000)	1408.0	768.0	1416.0
Crystal size/mm^3	0.21 × 0.16 × 0.15	0.2 × 0.14 × 0.12	0.89 × 0.71 × 0.59
Radiation	Mo K_α (λ = 0.71073)	Mo K_α (λ = 0.71073)	Mo K_α (λ = 0.71073)
2Θ range for data collection/°	5.284 to 54.206	4.912 to 54.506	4.52 to 50.274
Index ranges	-8 ≤ h ≤ 8, -16 ≤ k ≤ 18, -34 ≤ l ≤ 33	-11 ≤ h ≤ 10, -15 ≤ k ≤ 16, -19 ≤ l ≤ 18	-17 ≤ h ≤ 17, -19 ≤ k ≤ 19, -19 ≤ l ≤ 19
Reflections collected	19085	18461	63941
Independent reflections	5471 [R_{int} = 0.0588, R_{sigma} = 0.0782]	6174 [R_{int} = 0.0598, R_{sigma} = 0.0650]	12269 [R_{int} = 0.1271, R_{sigma} = 0.1127]
Data/restraints/parameters	5471/460/398	6174/0/434	12269/315/1027
Goodness-of-fit on F^2	1.147	1.079	1.052
Final R indexes [I>=2σ (I)]	R_1 = 0.0702, wR_2 = 0.1505	R_1 = 0.0884, wR_2 = 0.2434	R_1 = 0.0924, wR_2 = 0.2463
Final R indexes [all data]	R_1 = 0.1477, wR_2 = 0.1804	R_1 = 0.1133, wR_2 = 0.2605	R_1 = 0.1534, wR_2 = 0.2808
Largest diff. peak/hole / e Å^{-3}	1.03/-0.63	2.62/-0.91	3.64/-0.48

$^a R_1 = \Sigma||F_o| - |F_c||/\Sigma|F_o|$ and $wR_2 = |\Sigma w(|F_o|^2 - |F_c|^2)|/\Sigma|w(F_o)^2|^{1/2}$

Table S2: Selected Bond Lengths for 1, 2 and 3.

1		2		3	
Atom–Atom	**Length [Å]**	**Atom–Atom**	**Length [Å]**	**Atom–Atom**	**Length [Å]**
Co1–O1	2.039(7)	Co2–O7$^{\#1}$	2.014(5)	Co1–O5$^{\#1}$	2.115(9)
Co1–O4	2.050(7)	Co2–O8	2.024(5)	Co1–O16$^{\#2}$	2.201(3)
Co1–O6$^{\#1}$	2.020(6)	Co2–O6$^{\#2}$	2.036(5)	Co1–O3	2.049(9)
Co1–O7$^{\#1}$	2.048(7)	Co2–O5$^{\#3}$	2.119(5)	Co1–O15$^{\#2}$	2.171(3)
Co1–N2$^{\#2}$	2.046(7)	Co2–N3$^{\#4}$	2.065(6)	Co1–N2	2.132(3)
Co2–O2	2.007(7)	Co1–O1	2.043(5)	Co1–N1	2.157(3)
Co2–O3	2.073(7)	Co1–O3	2.033(5)	Co1–O4$^{\#1}$	2.002(11)
Co2–O5$^{\#1}$	2.058(7)	Co1–O4$^{\#5}$	2.021(4)	Co1–O2	2.018(9)
Co2–O8$^{\#1}$	2.031(7)	Co1–O2$^{\#5}$	2.053(5)	Co2–O11	2.009(9)
Co2–N1	2.053(7)	Co1–N1	2.060(5)	Co2–O14$^{\#3}$	2.060(9)
				Co2–O9	2.146(3)
				Co2–O8	2.205(3)
				Co2–N6	2.139(3)
				Co2–N4$^{\#4}$	2.142(3)
				Co2–O13$^{\#3}$	2.009(10)
				Co2–O12	2.012(9)

Table S3: Selected Bond Angles for 1, 2 and 3.

1		2		3	
Atom–Atom–Atom	**Angle [°]**	**Atom–Atom–Atom**	**Angle [°]**	**Atom–Atom–Atom**	**Angle [°]**
O1–Co1–O4	87.1(3)	O7$^{\#1}$–Co2–O8	166.26(19)	O5$^{\#1}$–Co1–O16$^{\#2}$	92.3(3)
O1–Co1–O7$^{\#1}$	87.3(3)	O7$^{\#1}$–Co2–O6$^{\#2}$	93.8(2)	O5$^{\#1}$–Co1–O15$^{\#2}$	152.5(3)
O1–Co1–N2$^{\#2}$	92.4(3)	O7$^{\#1}$–Co2–O5$^{\#3}$	86.2(2)	O5$^{\#1}$–Co1–N2	89.7(3)
O6$^{\#1}$–Co1–O1	165.7(3)	O7$^{\#1}$–Co2–N3$^{\#4}$	96.1(2)	O5$^{\#1}$–Co1–N1	89.0(3)
O6$^{\#1}$–Co1–O4	91.7(3)	O8–Co2–O6$^{\#2}$	89.4(2)	O3–Co1–O5$^{\#1}$	118.5(5)
O6$^{\#1}$–Co1–O7$^{\#1}$	90.7(3)	O8–Co2–O5$^{\#3}$	87.6(2)	O3–Co1–O16$^{\#2}$	149.1(5)
O6$^{\#1}$–Co1–N2$^{\#2}$	101.9(3)	O8–Co2–N3$^{\#4}$	96.3(2)	O3–Co1–O15$^{\#2}$	88.7(5)
O7$^{\#1}$–Co1–O4	166.4(3)	O6$^{\#2}$–Co2–O5$^{\#3}$	166.6(2)	O3–Co1–N2	92.4(4)
N2$^{\#2}$–Co1–O4	97.2(3)	O6$^{\#2}$–Co2–N3$^{\#4}$	101.9(2)	O3–Co1–N1	85.5(4)
N2$^{\#2}$–Co1–O7$^{\#1}$	95.4(3)	N3$^{\#4}$–Co2–O5$^{\#3}$	91.5(2)	O15$^{\#2}$–Co1–O16$^{\#2}$	60.38(10)
O2–Co2–O3	90.2(3)	O1–Co1–O2$^{\#5}$	168.2(2)	N2–Co1–O16$^{\#2}$	90.87(12)
O2–Co2–O5$^{\#1}$	166.7(3)	O1–Co1–N1	100.0(2)	N2–Co1–O15$^{\#2}$	93.00(12)
O2–Co2–O8$^{\#1}$	91.9(3)	O3–Co1–O1	88.38(19)	N2–Co1–N1	176.67(13)
O2–Co2–N1	101.4(3)	O3–Co1–O2$^{\#5}$	89.78(19)	N1–Co1–O16$^{\#2}$	92.24(12)
O5$^{\#1}$–Co2–O3	88.2(3)	O3–Co1–N1	95.6(2)	N1–Co1–O15$^{\#2}$	89.57(12)
O8$^{\#1}$–Co2–O3	165.7(3)	O4$^{\#5}$–Co1–O1	89.72(19)	O4$^{\#1}$–Co1–N2	94.0(3)
O8$^{\#1}$–Co2–O5$^{\#1}$	86.5(3)	O4$^{\#5}$–Co1–O3	168.35(19)	O4$^{\#1}$–Co1–N1	84.5(3)
O8$^{\#1}$–Co2–N1	97.3(3)	O4$^{\#5}$–Co1–O2$^{\#5}$	89.7(2)	O4$^{\#1}$–Co1–O2	113.7(5)
N1–Co2–O3	96.2(3)	O4$^{\#5}$–Co1–N1	96.1(2)	O2–Co1–N2	88.4(4)
N1–Co2–O5$^{\#1}$	91.9(3)	O2$^{\#5}$–Co1–N1	91.8(2)	O2–Co1–N1	89.5(4)
				O11–Co2–O9	152.0(5)

Table S4: The shape analysis for 1 and 2

1	PP-5	D_{5h}	Pentagon
2	vOC-5	C_{4v}	Vacant octahedron
3	TBPY-5	D_{3h}	Trigonal bipyramid
4	SPY-5	C_{4v}	Spherical square pyramid
5	JTBPY-5	D_{3h}	Johnson trigonal bipyramid J12

Coordination polymer **1**

Structure [ML_5]	**PP-5**	**vOC-5**	**TBPY-5**	**SPY-5**	**JTBPY-5**
Co 1	31.326	**0.459**	5.851	0.585	7.771
Co 2	31.259	**0.447**	6.035	0.574	8.051

Coordination polymer **2**

Structure [ML_5]	**PP-5**	**vOC-5**	**TBPY-5**	**SPY-5**	**JTBPY-5**
Co 1	31.002	**0.362**	6.191	0.667	8.015
Co 2	31.565	**0.463**	6.149	0.631	7.780

Table S5: The shape analysis for 3

1	HP-6	D_{6h}	Hexagon
2	PPY-6	C_{5v}	Pentagonal pyramid
3	OC-6	O_h	Octahedron
4	TPR-6	D_{3h}	Trigonal prism
5	JPPY-6	C_{5v}	Johnson pentagonal pyramid J2

Structure [ML_6]	**HP-6**	**PPY-6**	**OC-6**	**TPR-6**	**JPPY-6**
Co1	33.939	22.659	**2.918**	10.129	26.866
Co2	33.938	22.656	**2.918**	10.129	26.863

^{1}H-NMR of Ligand (L): ^{1}H-NMR (500 MHz, $CDCl_3$): δ = 8.78 (d, 4H, CH=N), 8.07 (d, 4H, ArH), 7.99 (s, 2H, ArH), 7.70 (d, 2H, ArH), 7.07 (d, 2H, ArH), 3.89 (s, 3H, CH_3-O) ppm.

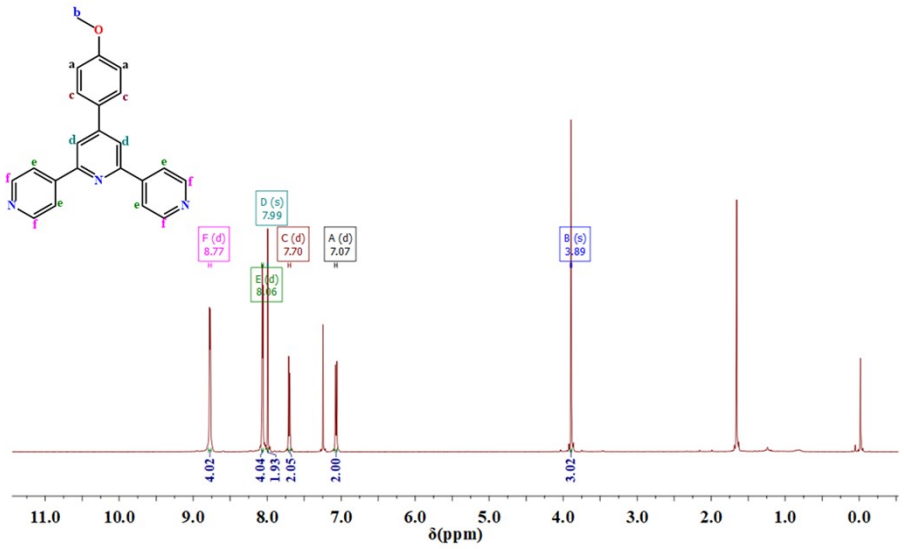

Fig. S1: ^{1}H-NMR of Ligand (L)

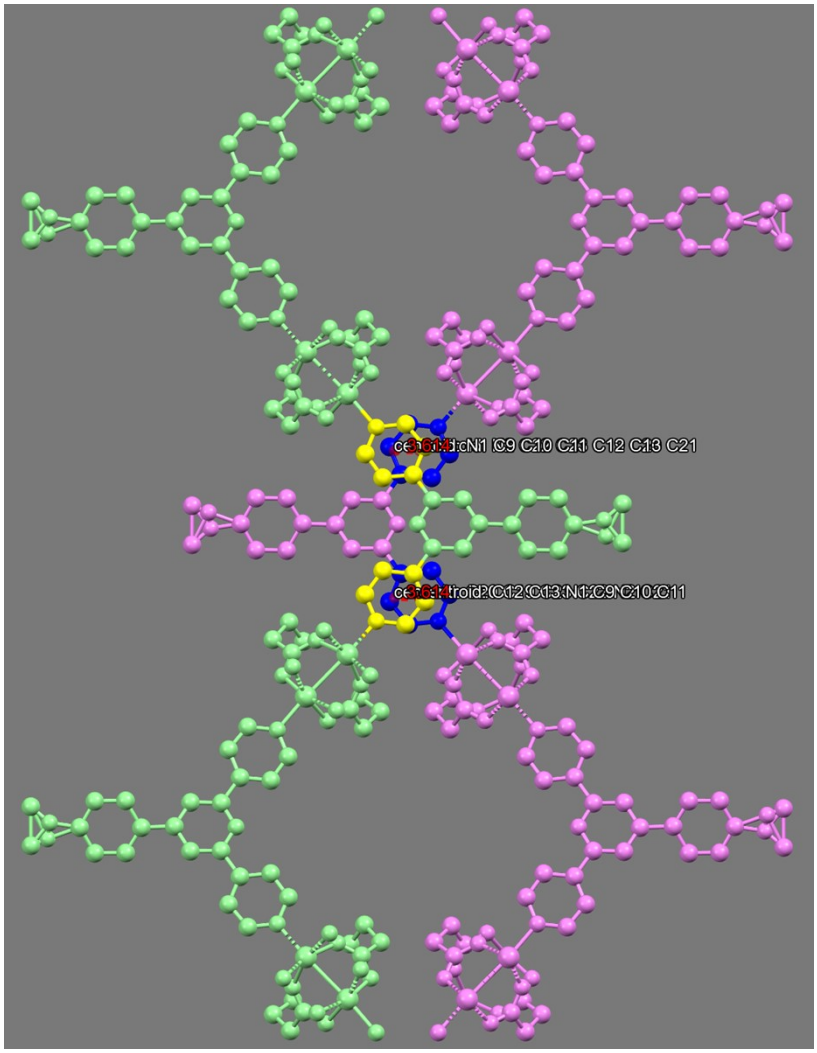

Fig. S2. π–π stacking between the benzene rings of **L** of two different sheet of **2**.

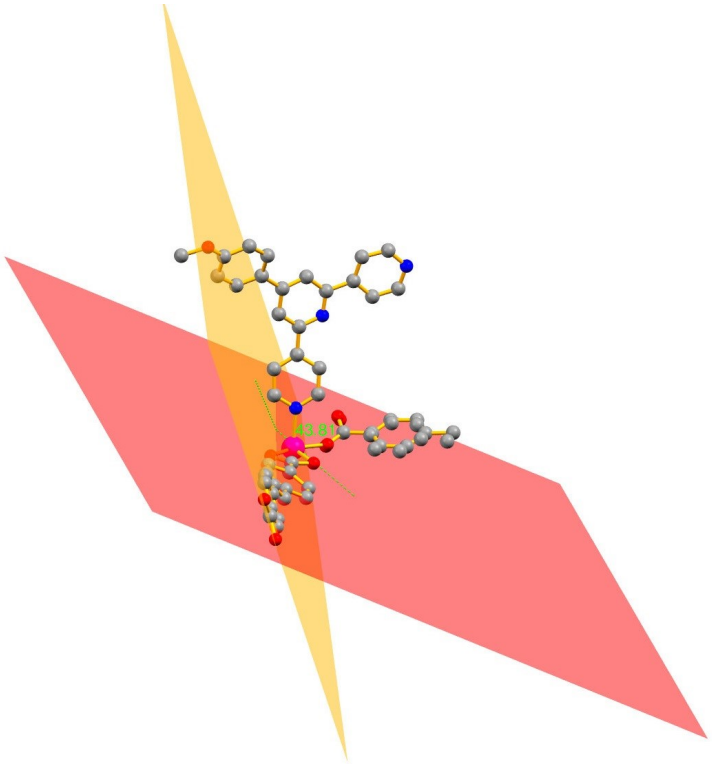

Fig. S3. The dihedral angle (43.81°) between the two phenyl rings of the $STdca^{-2}$ in **3**.

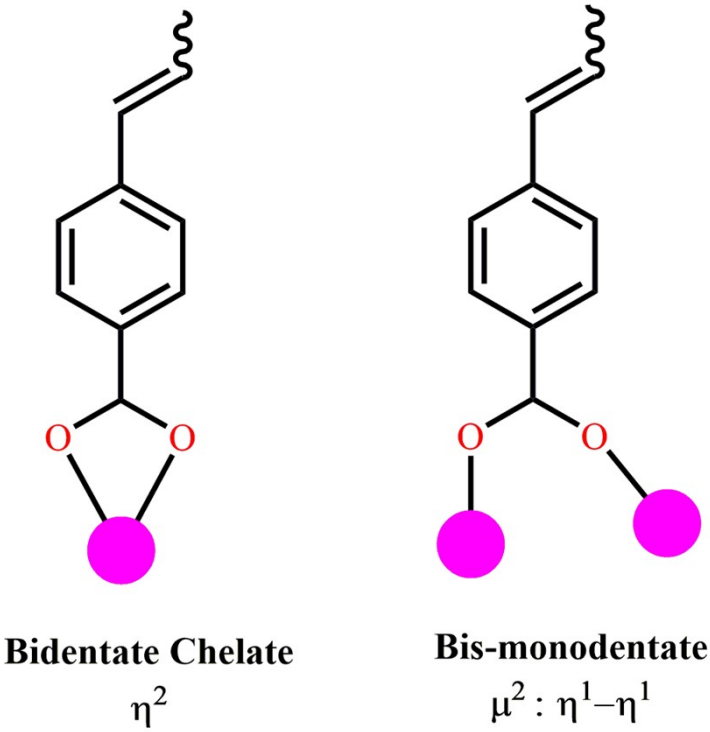

Fig. S4. Binding mode of the $STdca^{2-}$ in **3**.

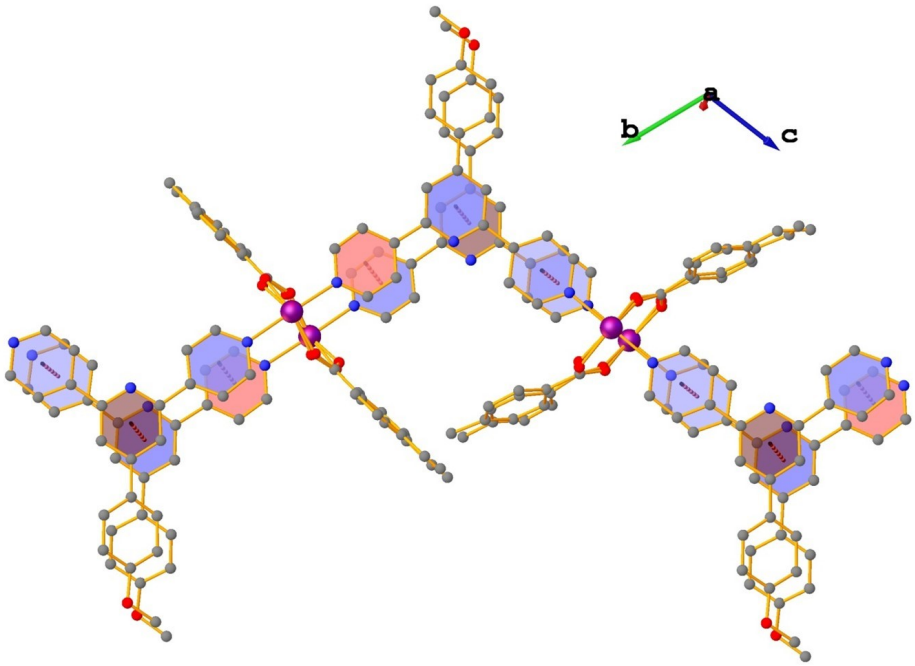

Fig. S5. π–π stacking between the benzene rings of **L** in **3**.

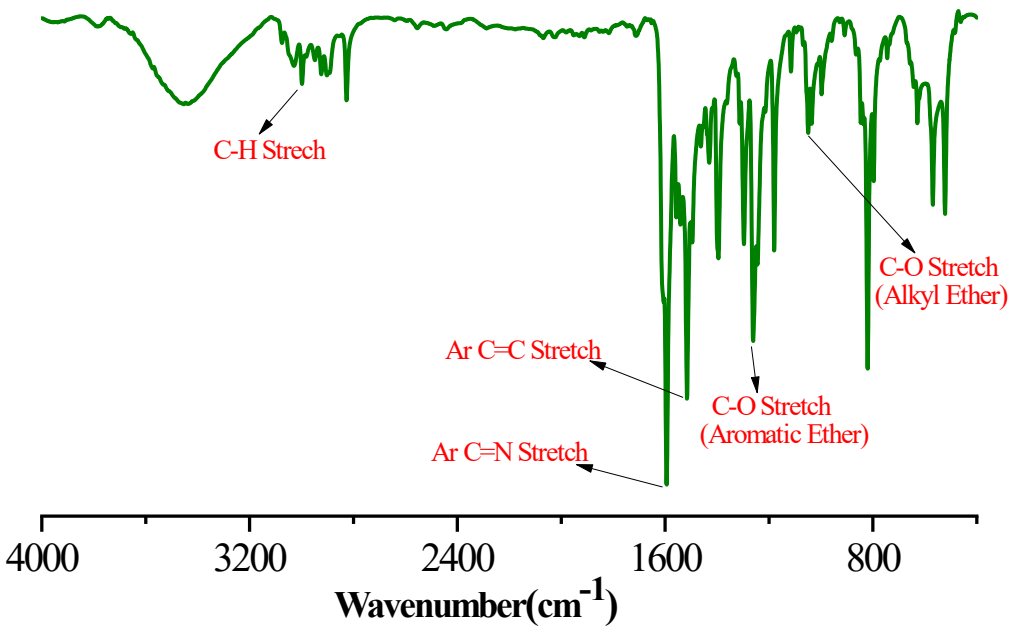

Fig. S6(a): FT-IR spectrum of Ligand (**L**).

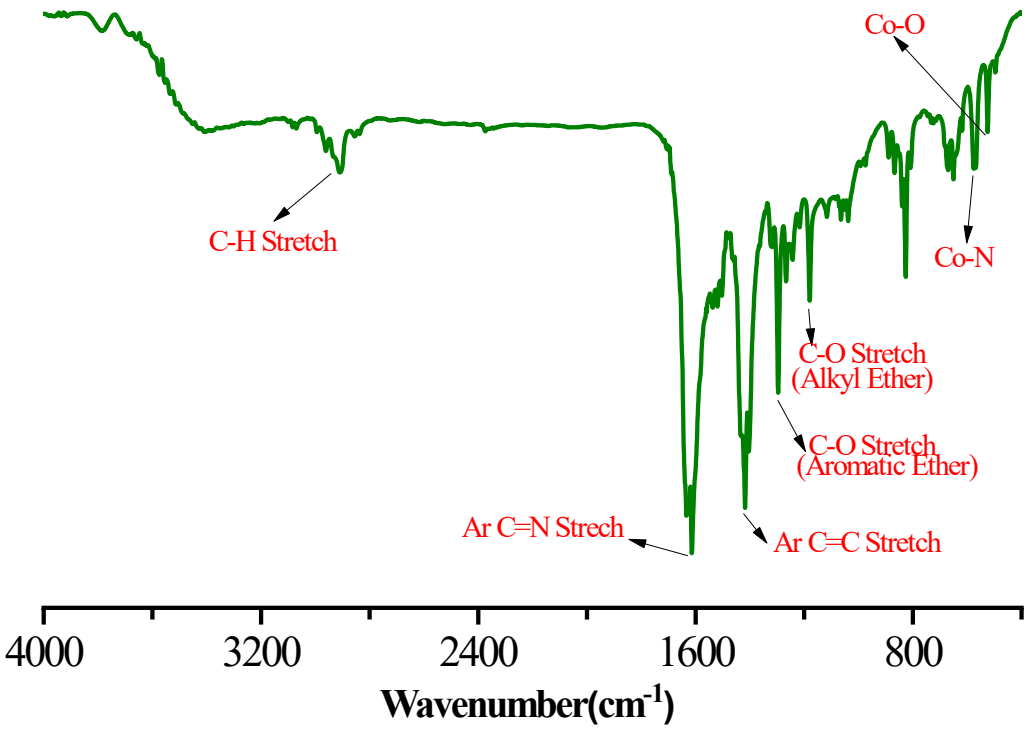

Fig. S6(b): FT-IR spectrum of **1**.

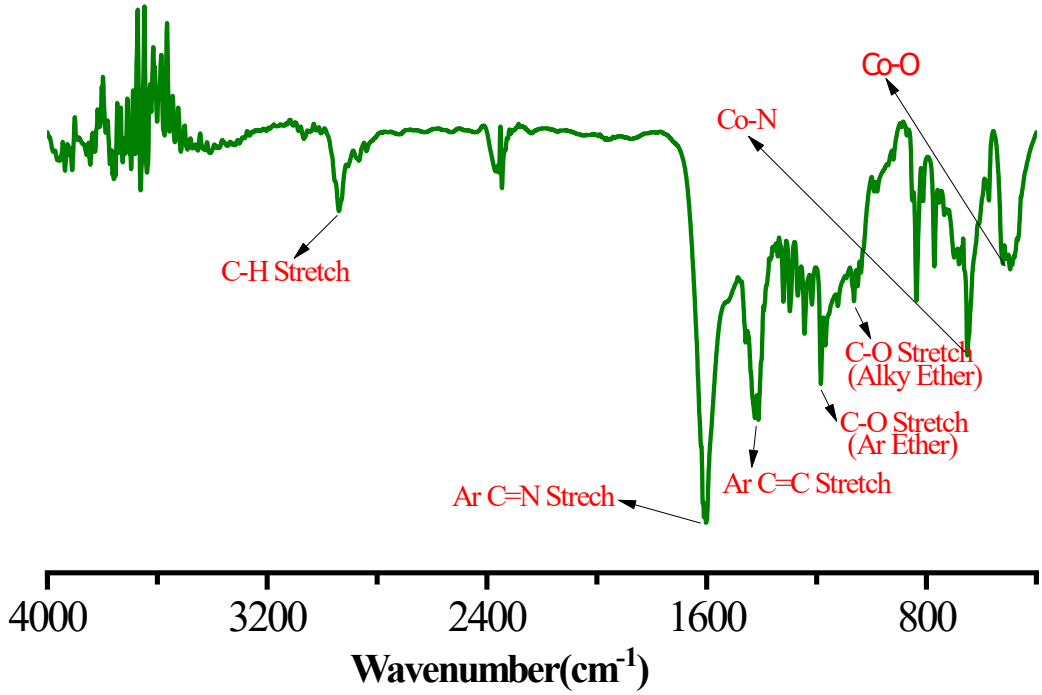

Fig. S6(c): The FT-IR spectrum of **2**.

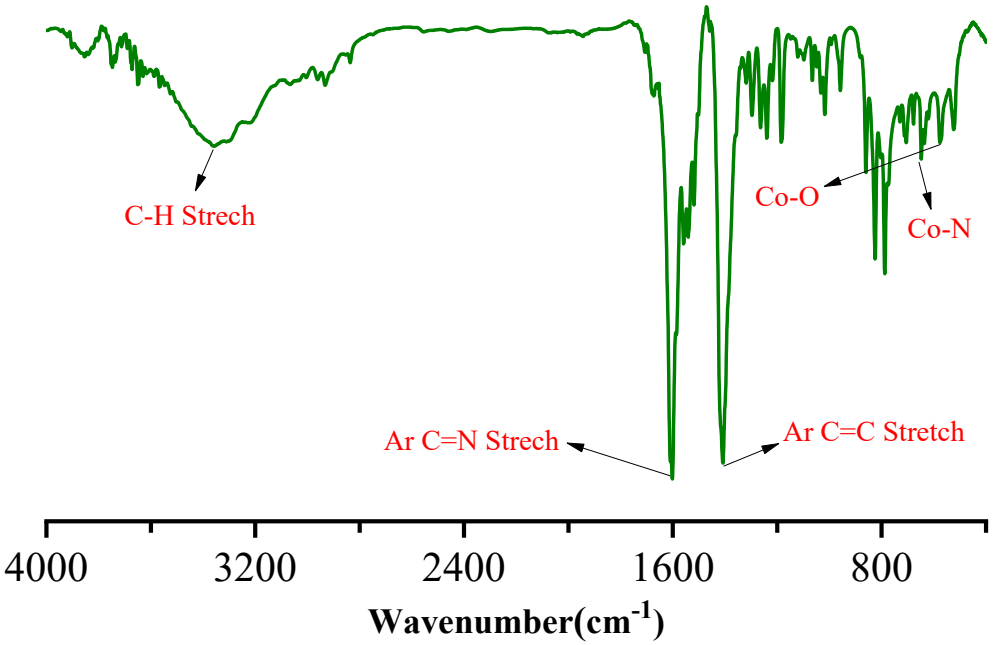

Fig. S6(d): The FT-IR spectrum of **3**.

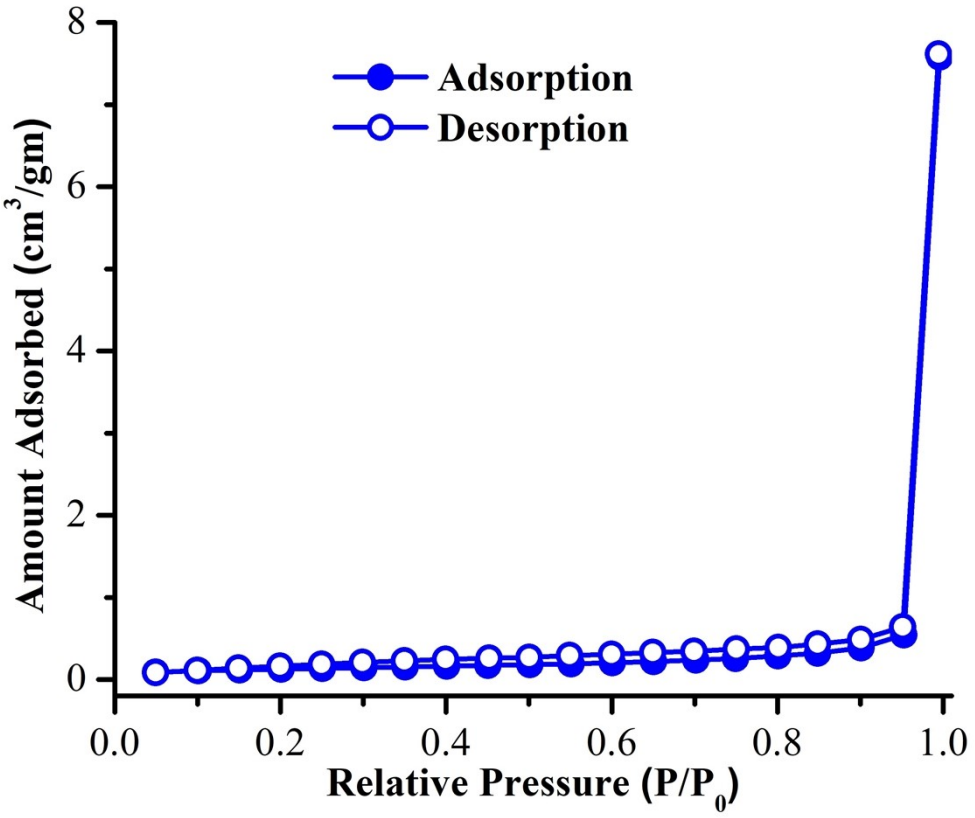

Fig. S7: N_2 adsorption isotherm for **3** at 77 K and 1 atm.

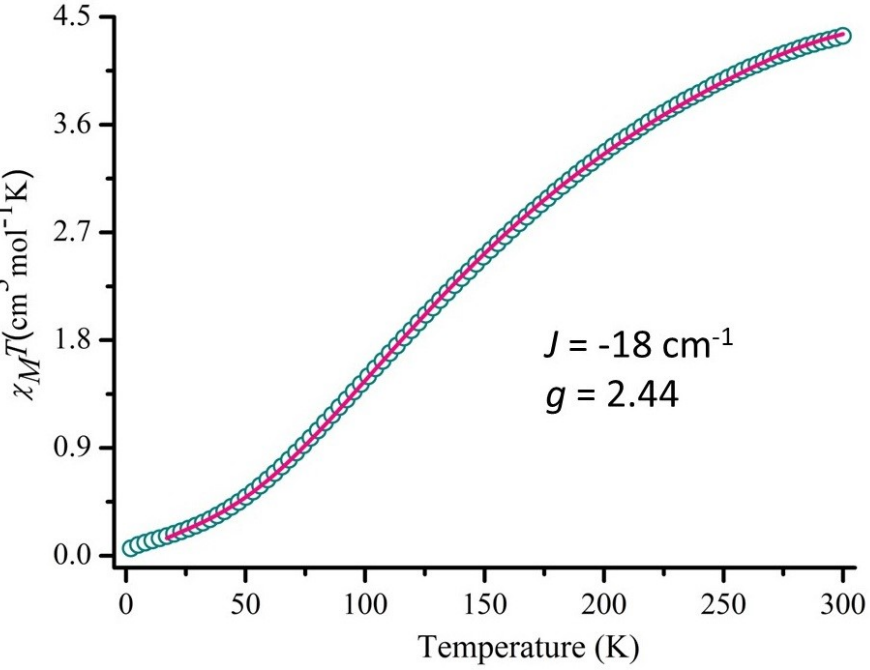

Fig. S8: Thermal dependence of the $\chi_M T$ product for **2** measured at 1 kOe.

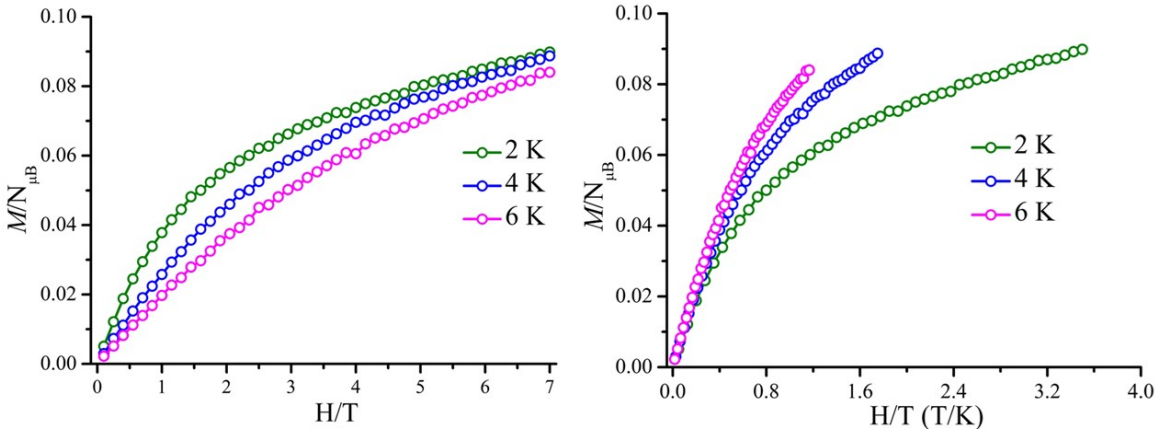

Fig. S9: *M*/NμB *vs.* H plot for **1** (left side) at the indicated temperatures, and reduced magnetization plot (right side).

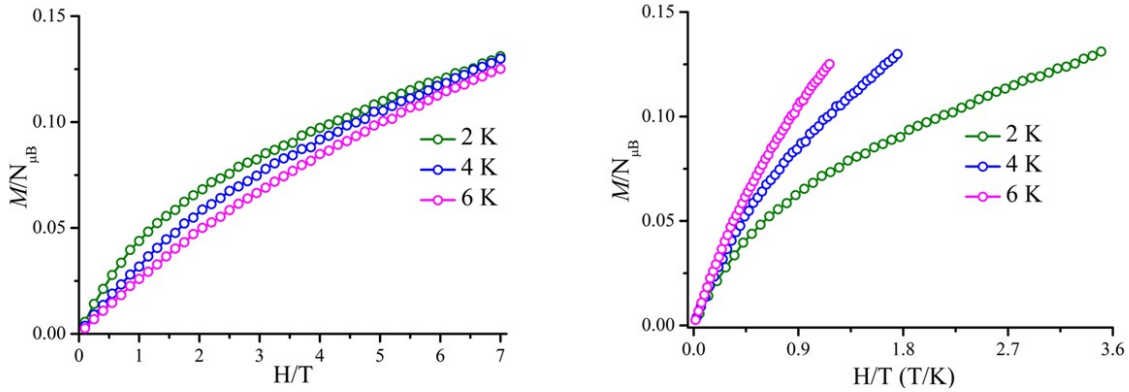

Fig. S10: *M*/NμB *vs.* H plot for **2** (left side) at the indicated temperatures, and reduced magnetization plot (right side).

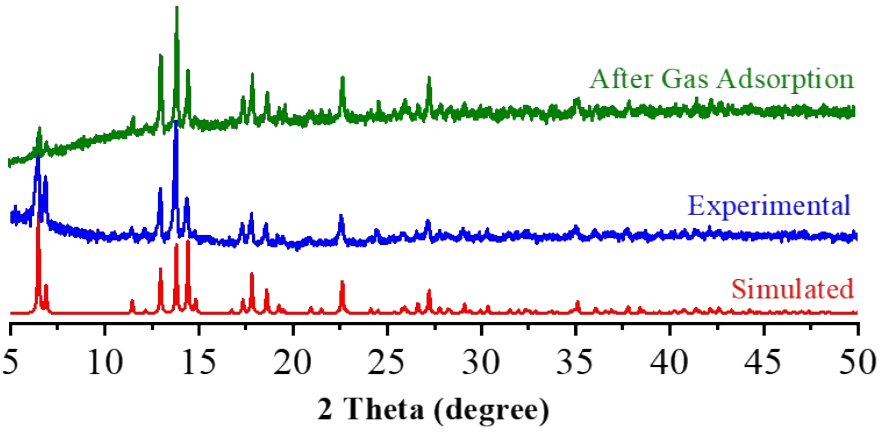

Fig. S11(a) The PXRD patterns of **CP-1** simulated from X-ray single-crystal data, as synthesized products and after BET measurements.

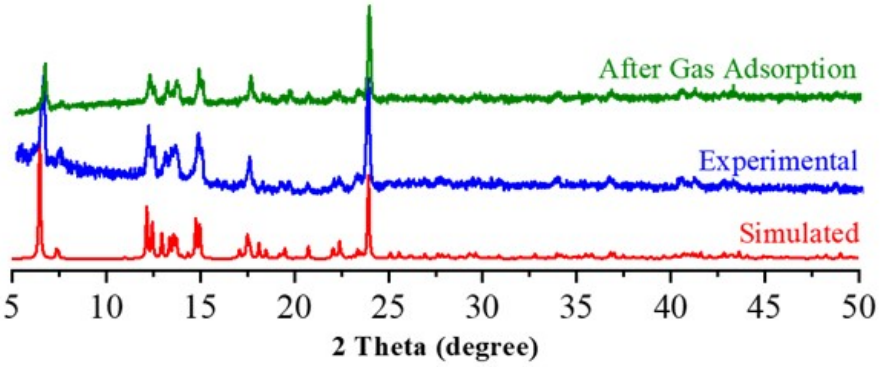

Fig. S11(b) The PXRD patterns of **CP2** simulated from X-ray single-crystal data, as synthesized products and after BET measurements.

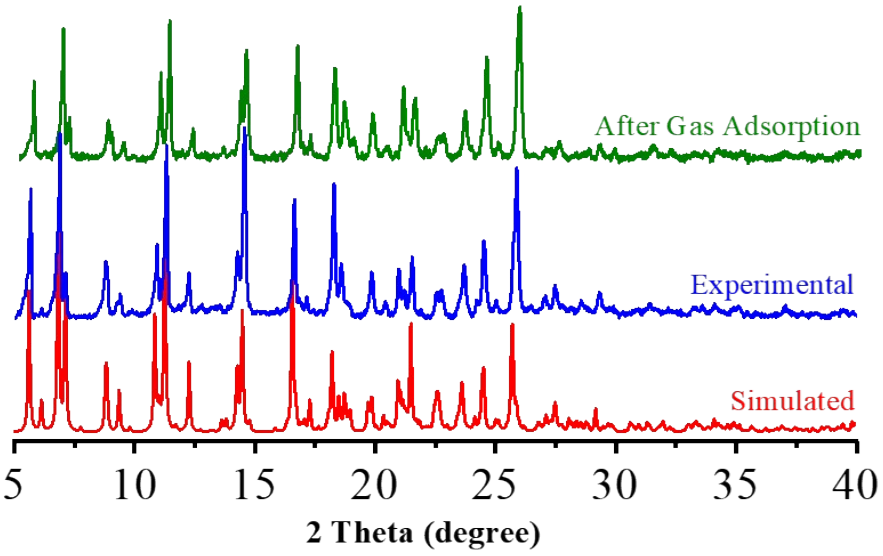

Fig. S11(c) The PXRD patterns of **CP3** simulated from X-ray single-crystal data, as synthesized products and after BET measurements.

Chemical Stability of the Frameworks of Coordination Polymers 1-3

The chemical stability of the three coordination polymers, CPs **1-3** were evaluated in terms of both solvent and pH tolerance. The stability of CPs **1-3** toward different organic solvents were evaluated by immersing the as synthesized samples in several common organic solvents, including water, ethanol (EtOH), dichloromethane (DCM), and hexane for 24 h. The samples were filtered and dried for PXRD measurements, and the results show that the PXRD patterns are almost perfectly consistent with the simulated one, from the single crystal X-ray data demonstrating the excellent solvent stability of CP **1-3** in different organic solvents (Figure S13). Furthermore, the acid-base stability of CPs **1-3** were evaluated. Samples were immersed in various pH (3–12) aqueous solutions for 24 h at room temperature, and the collected dried samples were characterized by PXRD analysis (Fig.S12). The resulting patterns are consistent with simulated ones, suggesting that CPs **1-3** possess good stability in acidic and strongly basic conditions (pH 3 & 12) are limiting its applicability under extreme environments however minor peak broadening was observed for CP **2** under strongly acidic conditions (pH 3), whereas CP **1** and **3** remained unchanged, highlighting its superior stability.

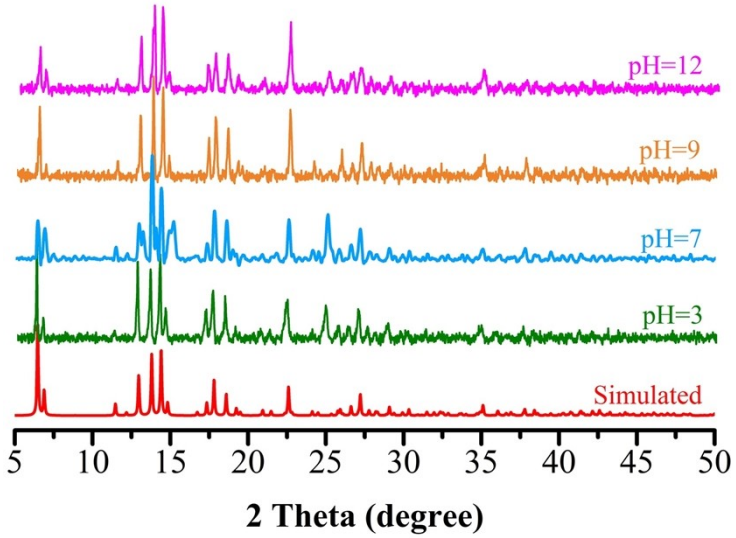

Fig. S12(a) The PXRD patterns of **1** showing the stability of framework under different pH.

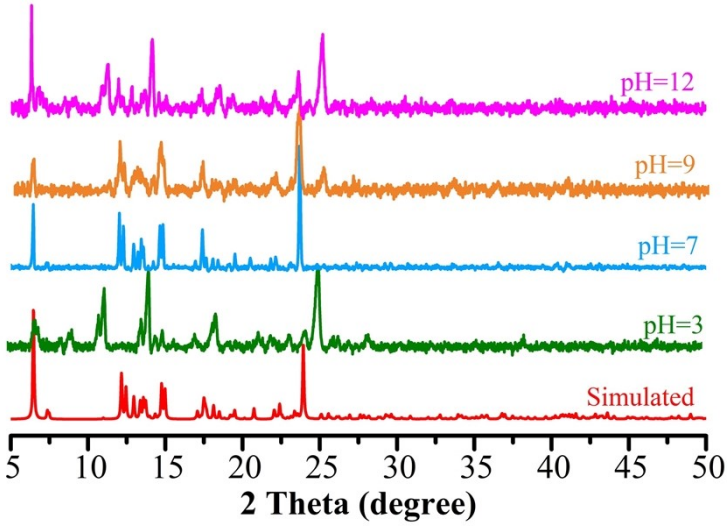

Fig. S12(b) The PXRD patterns of **2** showing the stability of framework under different pH.

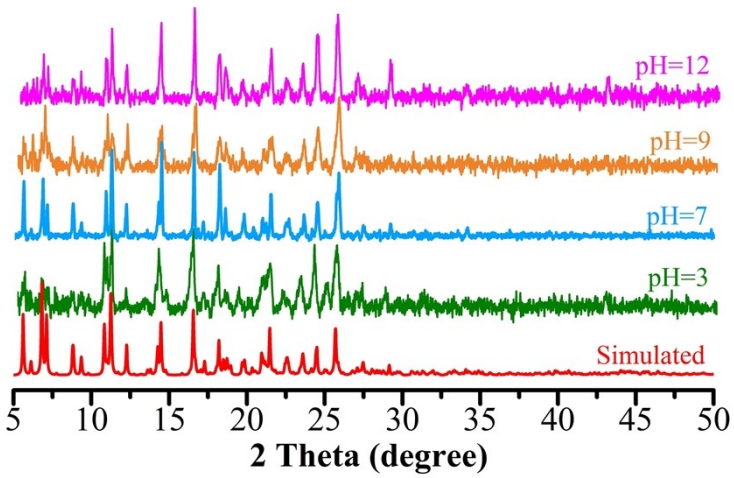

Fig. S12(c) The PXRD patterns of **3** showing the stability of framework under different pH.

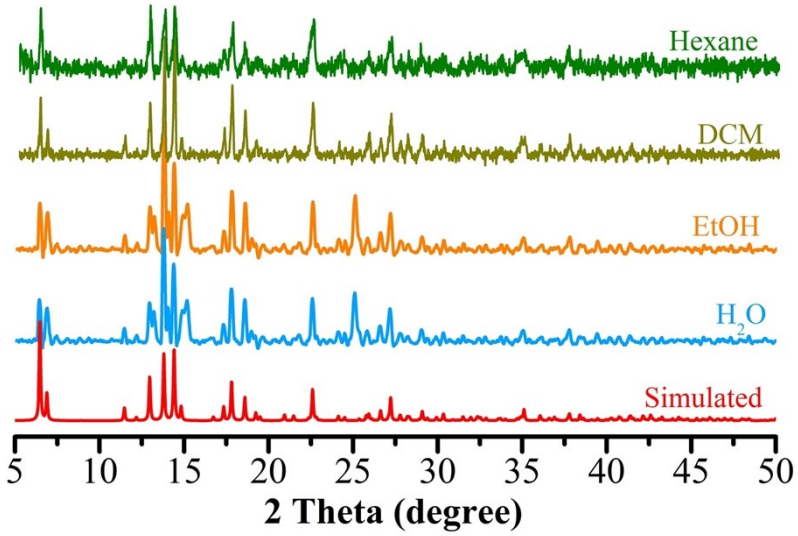

Fig. S13(a) The PXRD patterns of **1** showing the stability of framework in different solvents.

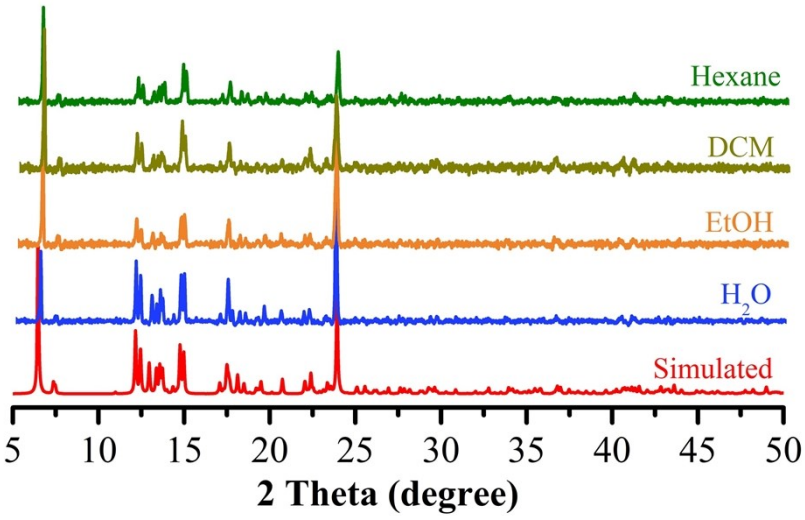

Fig. S13(b) The PXRD patterns of **2** showing the stability of framework in different solvents.

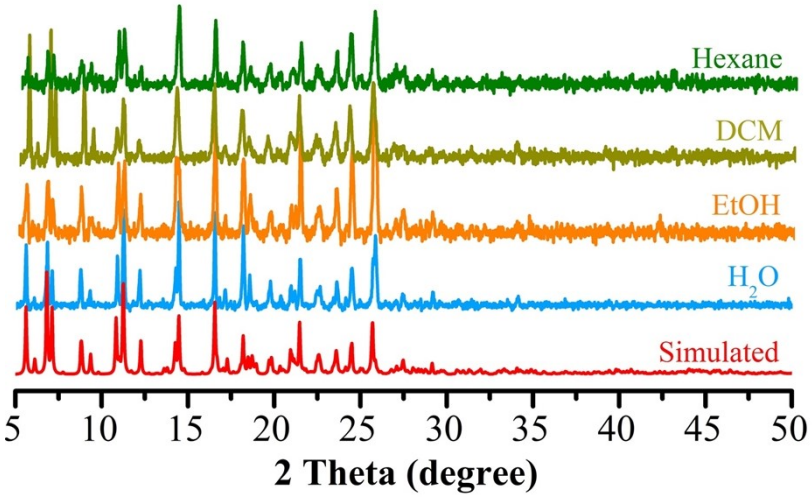

Fig. S13(c) The PXRD patterns of **3** showing the stability of framework in different solvents.